Generation of Monomeric Reversibly Switchable Red Fluorescent Proteins for Far-Field Fluorescence Nanoscopy

Andre C. Stiel, Martin Andresen, Hannes Bock, Michael Hilbert, Jessica Schilde, Andreas Schönle, Christian Eggeling, Alexander Egner, Stefan W. Hell, and Stefan Jakobs
Department of NanoBiophotonics, Max Planck Institute for Biophysical Chemistry, Göttingen, Germany

ABSTRACT   Reversibly switchable fluorescent proteins (RSFPs) are GFP-like proteins that may be repeatedly switched by irradiation with light from a fluorescent to a nonfluorescent state, and vice versa. They can be utilized as genetically encodable probes and bear large potential for a wide array of applications, in particular for new protein tracking schemes and subdiffraction resolution microscopy. However, the currently described monomeric RSFPs emit only blue-green or green fluorescence; the spectral window for their use is thus rather limited. Using a semirational engineering approach based on the crystal structure of the monomeric nonswitchable red fluorescent protein mCherry, we generated rsCherry and rsCherryRev. These two novel red fluorescent RSFPs exhibit fluorescence emission maxima at ~610 nm. They display antagonistic switching modes, i.e., in rsCherry irradiation with yellow light induces the off-to-on transition and blue light the on-to-off transition, whereas in rsCherryRev the effects of the switching wavelengths are reversed. We demonstrate time-lapse live-cell subdiffraction microscopy by imaging rsCherryRev targeted to the endoplasmic reticulum utilizing the switching and localization of single molecules.

INTRODUCTION

Fluorescent proteins (FPs) glowing in all hues, have become indispensable research tools in cellular biology (1–3). Recently, novel FPs have been described which may be reversibly photoswitched between a fluorescent and a nonfluorescent state (4,5). Such reversibly switchable fluorescent proteins (RSFPs) have already been used for innovative protein tracking strategies (6), for fluorescence correlation spectroscopy at high molecular concentrations (7), and within different schemes to facilitate subdiffraction imaging in far-field optical microscopy (8–13).

In RSFPs, photoinduced reversible switching from the nonfluorescent to the fluorescent state, and vice versa, is achieved by irradiation with light of different wavelengths, where the light of one wavelength in addition to switching also excites fluorescence. A positive and a negative switching mode may be distinguished: In a positive-switching RSFP, the wavelength used to excite fluorescence switches the protein to the on-state. In case of a RSFP with a negative-switching mode, the wavelength used to excite fluorescence concurrently induces the on-to-off transition. In each case, the respective other transition is induced by light of a shorter wavelength. In contrast to photoactivatable fluorescent proteins (14), the photoswitching of RSFPs is reversible and the fluorophores may pass the switching cycle many times until they are photo-destroyed or transferred to a permanent nonswitchable state.

Recent studies into the molecular switching mechanism of RSFPs demonstrated that a *cis-trans* isomerization of the chromophore is a key event in the switching process (15–19).

In the RSFPs studied so far, the *cis*-conformation represents the fluorescent on-state, whereas the chromophore in the nonfluorescent off-state adopts the *trans*-conformation. The conformational changes are accompanied by different protonation equilibria of the chromophore (20–22). The different protonation equilibria determine the absorption spectra of the chromophore in both states. The on-state chromophores were found to be well ordered and relatively planar, whereas the off-state chromophores were more twisted and partially disordered, a condition likely to favor nonradiative decay of the excited chromophore.

The available monomeric RSFPs emit blue-green or green fluorescence (5,19,23). They all display negative-switching modes. Of these green fluorescent RSFPs, Dronpa and its variants are the most prominent (5,18,24), and have been used for several applications. The only known red fluorescent RSFP is asFP595 and its variants (4,25), but since asFP595 is an obligate tetramer, its practical use is limited. The current lack of monomeric RSFPs emitting yellow or red light prevents the utilization of RSFPs in dual-color experiments, representing a severe hurdle for their widespread use.

A promising area of application for RSFPs of various colors is far-field subdiffraction resolution microscopy. Every far-field fluorescence microscopy concept that has successfully outperformed diffraction is based on the switching between at least two molecular states, one of which is dark while the other gives a signal (13). Initial subdiffraction concepts following this pathway utilized reversible saturable optical linear (fluorescence) transitions (RESOLFT) with a beam of light featuring a local intensity minimum (26–29). The more recent superresolution concepts based on the readout of stochastically switched-on isolated single molecules have been termed PALM (10), STORM (30), fPALM

(31), and PALMIRA (12). PALMIRA uses an asynchronous acquisition mode in which readout and photoswitching are independently operated, which substantially reduces the acquisition time. To utilize fluorescent proteins within a RESOLFT approach, reversible switching is indispensable, whereas in the single molecule superresolution concepts reversibility is not essential but may be particularly useful for dynamic experiments in which several images must be acquired sequentially.

To expand the available set of monomeric RSFPs, we set out to generate RSFPs emitting red light. Based on the reported switching mechanism, we chose a semirational design approach to transform the monomeric red fluorescent protein mCherry (3) into a reversibly photoswitchable fluorescent protein. Thereby we generated two novel RSFPs, rsCherry and rsCherryRev, which emit light at $\lambda \sim 610$ nm and display positive and negative switching modes, respectively. We show the use of rsCherryRev for time-lapse live-cell subdiffraction resolution microscopy in mammalian cells.

MATERIALS AND METHODS

Mutagenesis

For site-directed random mutagenesis, the QuikChange Site Directed Mutagenesis Kit (Stratagene, La Jolla, CA) or a multiple-site mutagenesis approach using several degenerate primers were used (32). Error-prone random mutagenesis was essentially performed as described (33). For expression in *Escherichia coli*, the coding sequences were cloned into a pQE30 vector (Qiagen, Hilden, Germany).

Protein production and purification

Proteins were expressed in the *E. coli* strain BL21-CP-RIL and purified by Ni-NTA affinity chromatography (Ni-NTA Spin Kit, Qiagen), according to the manufacturer's instructions. The purified proteins were concentrated by ultrafiltration and taken up in 100 mM Tris-HCl, 150 mM NaCl, pH 7.5.

Expression in mammalian cells

To target rsCherryRev to the lumen of the endoplasmic reticulum (ER), the coding sequence was amplified by PCR using the primers

CTGCAGGTCGACATGGTGAGCAAGGGCGAGGA

and

TTCTGCGGCCGCCTTGTACAGCTCGTCCATGCCG CCGGT.

The PCR fragments were digested with *Sal*I and *Not*I and inserted into the vector pEF/myc/ER (Invitrogen, Carlsbad, CA). The resultant fusion proteins are directed to the ER and then retained in this organelle. For the generation of α-tubulin fusion constructs, the rsCherryRev coding sequence was amplified by PCR using the primers

GATCCGCTAGCGCTAATGGTGAGCAAGGGCGAG GAG

and

CACTCGAGATCTGAGTCCGGACTTGTACAGCTCG TCCATGCC.

The PCR fragments were digested with *Nhe*I and *Bgl*II and inserted into the vector pEGFP-Tub (Clontech, Mountain View, CA), replacing the EGFP sequence.

The plasmids were transfected into mammalian PtK2 (*Potorous tridactylis*) cells using the Nanofectin Kit (PAA, Pasching, Austria) according to the manufacturer's instructions. The cells were propagated in DMEM medium with GlutaMAX and 4.5 g/L glucose, 10% (v/v) BSA, 1 mM sodium pyruvate, 50 μg/mL penicillin, and 50 μg/mL streptomycin. Cells were grown on coverslips in petri dishes at 37°C under 95% humidity and 7% CO_2.

Spectroscopic analysis and optical switching

The absorption and fluorescence spectra of purified proteins were recorded with a Varian Cary 4000 UV/VIS photospectrometer and a modified Varian Cary Eclipse fluorescence spectrometer (Varian, Palo Alto, CA), respectively. The absorption spectra were recorded at thermal equilibrium.

All switching curves were determined on colonies of live *E. coli* cells expressing the respective proteins. The photoswitching experiments were performed using a modified computer-controlled fluorescence microscope (Leica, Wetzlar, Germany) equipped with a 40 × NA 0.6 air objective lens. The microscope was equipped with two 100 W Hg lamps delivering yellow light (550 ± 20 nm excitation filter, ~2 W/cm^{-2}) and blue light (450 ± 20 nm excitation filter, ~4 W/cm^{-2}). For photoswitching of both rsCherry and rsCherryRev, irradiation was performed in alternate turns with yellow light for 12 s and yellow + blue light for 0.5 s. The fluorescence was detected through the same objective lens and recorded by a photomultiplier tube (HR9306-0, Hamamatsu, Hamamatsu City, Japan) using a 600 nm long-pass detection filter (HQ 600 LP, AHF Analysentechnik, Tübingen, Germany).

The relaxation half-time $t_{1/2}^{on-relax}$ from the ensemble on-state into the thermal equilibrium state was measured on colonies of *E. coli* cells expressing rsCherry or rsCherryRev, respectively. After switching into the on-state (to the maximal attainable fluorescence signal) with yellow light (550 ± 20 nm excitation filter, ~6 W/cm^{-2}) for 2 s (rsCherry) or with blue light (450 ± 20 nm excitation filter, ~4 W/cm^{-2}) for 2 s (rsCherryRev), the relaxation into the equilibrium state was followed at room temperature (22°C) in the dark by consecutive short measurements (0.02 s) with yellow light (~0.5 W/cm^{-2}) every 20 s or 2 s for rsCherry or rsCherryRev, respectively. For the determination of $t_{1/2}^{on-relax}$ of rsCherryRev (Fig. 2 *E*), the *E. coli* colony utilized for the measurement was initially optically switched >10 times (see also Supplementary Material Fig. S3 in Data S1).

Dynamic light scattering analysis

Dynamic light scattering analysis was carried out using a DynaPro-MS/X (Wyatt Technology, Santa Barbara, CA) molecular-sizing instrument at 25°C. For the measurement, a 50 μL sample was passed through a filtering assembly containing a 0.2 μm filter into a 12 μL chamber quartz cuvette. The data were analyzed using the Dynamics 6.0 software. mCherry was taken as monomer as in Shaner et al. (3).

Size separation chromatography

The proteins (1 mg/ml^{-1}, in 100 mM Tris-HCl, 150 mM NaCl, pH 7.5) were analyzed on a Superdex 200 column with a Smart system (both Pharmacia, Uppsala, Sweden). Flow was set to 40 μL/min^{-1} and the absorption at 280 nm was monitored continuously. Chromatography was performed at room temperature.

Brightness determination

We determined two different types of brightness values, based either on an ensemble of molecules or on single proteins. Ensemble brightness values were determined using the optical switching setup described above. We prepared solutions of purified proteins in 100 mM Tris-HCl, 150 mM NaCl, pH 7.5 of equal concentrations (as determined by the absorption at 280 nm) and measured their fluorescence signal in the maximal attainable on-state (550 ± 20 nm excitation filter, ~ 2 W/cm^{-2}) relative to mCherry.

The brightness of a single protein was determined on solutions of purified proteins using fluorescence correlation spectroscopy (see also Fig. S2 in Data S1) (34). Fluorescence correlation data were recorded on a confocal microscope setup equipped with a 561 nm laser for fluorescence excitation (Cobolt, Solna, Sweden) and analyzed as outlined previously (7). The single molecule brightness values were defined as the average fluorescence count rate per light-emitting single molecule diffusing through the confocal detection volume.

Wide-field imaging

For imaging of *E. coli* cells, rsCherry and rsCherryRev were expressed in BL21-CP-RIL. *E. coli* cells expressing either of these proteins were mixed and imaged with a Leica DM6000 epifluorescence microscope (Leica, Wetzlar, Germany). The microscope was equipped with a $100 \times$ NA 1.40 oil immersion objective lens and a DFC350 FX camera (Leica). The 100 W Hg lamp delivered yellow light (546 ± 6 nm excitation filter, ~ 4 W/cm^{-2}) or blue light (470 ± 20 nm excitation filter, ~ 5 W/cm^{-2}). Fluorescence was recorded using a 600 ± 20 nm bandpass detection filter. The *E. coli* cells were imaged with the following irradiation scheme:

1. Switching for 1 s with yellow light (rsCherry: On; rsCherryRev: Off).
2. Imaging with yellow light excitation (60 ms).
3. Switching for 1 s with blue light (rsCherry: Off; rsCherryRev: On).
4. Imaging with yellow light excitation (60 ms).

For the imaging of rsCherryRev expressed in PtK2 cells, the same microscope as described above equipped with a BGR-Filter Cube (Leica), delivering yellow light (570 ± 10 nm excitation filter, ~ 15 W/cm^{-2}) or blue light (495 ± 7.5 nm excitation filter, ~ 6 W/cm^{-2}) was employed. A 640 ± 20 nm bandpass filter was used for detection. The following irradiation scheme was employed:

1. Switching for 1.1 s with blue light (rsCherryRev: On).
2. Imaging with yellow light excitation (160 ms).
3. Switching for 1.1 s with yellow light (rsCherryRev: Off).
4. Imaging with yellow light excitation (160 ms).

PALMIRA microscopy

The arrangement of the wide-field imaging setup utilized for subdiffraction PALMIRA microscopy was essentially as described earlier (12). In brief, the beam of a continuous-wave, diode-pumped solid-state laser running at 561 nm (Cobolt Jive 50; Cobolt, Stockholm, Sweden) was intensity-controlled by an acousto-optical tunable filter (AA-AOTF-nC, Pegasus Optik, Wallenhorst, Germany) and expanded by a telescope. The beam polarization was converted from linear to circular by a quarter wave-plate and subsequently coupled into a commercial wide-field microscope (DM IRB, Leica Microsystems, Mannheim, Germany). We achieved uniform epiillumination of an area of ~ 10-μm diameter by underilluminating the back aperture of the objective lens (HCX PL APO $100\times/1.4$ oil, Leica Microsystems). The fluorescence light was collected by the same lens, separated from the excitation light using a dichroic filter (zUV/561rpc, AHF Analysentechnik, Tübingen, Germany) and imaged onto an electron multiplying charge-coupled device camera (IXON-Plus DU-860, Andor Technology, Belfast, Northern Ireland). The detected wavelength range was limited to the emission spectrum of

rsCherryRev by a bandpass filter (620 ± 30 nm, Chroma Technology, Rockingham, VT). Before data acquisition, the majority of the proteins were switched to a dark state by illuminating the sample for ~ 1 min with 20 kW/cm^{-2} of the 561-nm laser light.

For each PALMIRA image, 20,000 frames were continuously recorded at a rate of 500 frames/s using 561-nm laser-light illumination at 20 kW/cm^{-2}. The background in each frame was estimated by applying a low-pass filter to the data. The planar positions of the individual rsCherryRev proteins in the background-corrected frames were determined by an implementation of Hogbom's classical CLEAN algorithm (35) in conjunction with a mask-fitting algorithm of the Airy spot as detailed previously (12).

The final PALMIRA images were obtained by depicting each fluorescent protein exhibiting >20 detected photons in a new frame as a Gaussian with a standard deviation corresponding to the respective localization accuracy (10). The epifluorescent (diffraction-limited) counterpart images to the superresolved PALMIRA images were determined by summing up all the signals of the background-corrected frames and interpolated to a pixel size of 40×40 nm. For display, we accounted for the comparatively high dynamic range in the images by selecting a color table which emphasizes dim features.

RESULTS

Generation of the red fluorescent reversibly photoswitchable protein rsCherry

To generate photoswitchable proteins emitting red fluorescence, we decided to use the fluorescent protein mCherry as a starting point. mCherry is a monomeric red fluorescent protein (Em.: 586 nm/ Exc.: 611 nm) with very good photostability that has been successfully employed in a number of live cell studies (3).

Like the chromophores of most fluorescent proteins, the chromophore of mCherry adopts a *cis*-conformation (PDB: 2H5Q) (36). Likewise, the on-state chromophores of all RSFPs analyzed so far are in the *cis*-position, whereas their respective off-state chromophores adopt a *trans*-position (16,17,19). Since the photoinduced *cis-trans* isomerization of the chromophore is a structural key event in the switching of RSFPs, we reasoned that to render mCherry switchable, it would be required to make the *trans*-position accessible to the chromophore. Modeling of a *trans* chromophore into the mCherry structure without adjusting the rest of the structure immediately revealed that Ile[161] (all amino-acid numbering according to the DsRed sequence) occupies the space required by a hypothetical *trans* chromophore (Fig. 1), thereby explaining the fact that the chromophore of mCherry is exclusively found in the fluorescent *cis*-conformation. We reasoned that exchange of Ile[161] by smaller amino-acid residues might make the *trans* position accessible to the chromophore and thus may facilitate photoinduced reversible switching.

We performed saturated site-directed mutagenesis at position 161. This resulted in mCherry-Ile[161]Ser. In *E. coli* colonies expressing this variant, fluorescence could be switched-off to $\sim 70\%$ of the initial brightness by irradiation with light of 450 nm. Irradiation with 550 nm brought the fluorescence back to the starting value. To improve the re-

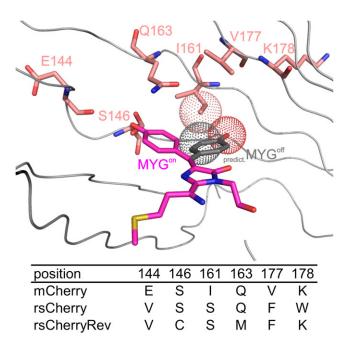| position	144	146	161	163	177	178
mCherry	E	S	I	Q	V	K
rsCherry	V	S	S	Q	F	W
rsCherryRev	V	C	S	M	F	K

FIGURE 1 Chromophore environment in mCherry with important amino-acid residues highlighted. Representation of the *cis*- (carbon atoms in *pink*) and the predicted (modeled) *trans*-chromophore (carbon atoms of the six-ring in *gray*) of mCherry (PDB: 2H5Q) (36). Without further amino-acid residue rearrangements, the predicted *trans*-chromophore would sterically interfere with the side chain of Ile[161] as indicated by the overlapping dotted van der Waals spheres. Amino-acid residues important to the generation of rsCherry or rsCherryRev are depicted as sticks. Ser[146] adopts two alternative conformations. The inset table lists all amino-acid residue exchanges in rsCherry and rsCherryRev.

versible switching characteristics, in particular to reduce the fluorescence signal in the off-state of mCherry-Ile[161]Ser, we performed PCR-based multiple-site mutagenesis at amino-acid positions spatially close to the chromophore, alternating with error-prone mutagenesis. After several rounds of mutagenesis, mCherry-Glu[144]Val, Ile[161]Ser, Val[177]Phe, Lys[178]Trp emerged as the so-far best reversibly switchable variant (Fig. 2 *A*, Table 1). All three additional mutations affect amino-acid residues in the vicinity of the chromophore. Hence, they might affect the stability of the chromophore or interfere with the energy barrier for switching (Fig. 1). Because of its favorable switching characteristics, we denote this variant as rsCherry (for reversibly switching Cherry).

Dynamic light scattering analysis and size exclusion chromatography verified that rsCherry is a monomer in solution (Table S1 and Fig. S1 in Data S1). In the fluorescent on-state, rsCherry exhibits an absorption peak at 572 nm and emits at 610 nm, hence the absorption spectrum is slightly blue-shifted compared to mCherry (Fig. 2 *C*, Table 1). It displays positive-switching characteristics, because irradiation with light of a wavelength that induces fluorescence (550 nm) converts the protein from the off- to the on-state, whereas irradiation with a shorter wavelength (450 nm) converts it from the on- to the off-state. Compared to

mCherry-Ile[161]Ser, the switching contrast has improved: In the off-state, *E. coli* cells expressing rsCherry display 15% of the fluorescence signal attainable in the on-state. The switching is reversible, although, upon multiple switching cycles of rsCherry in *E. coli*, we observed an increase in the residual fluorescence signal when the molecules were switched into the off-state, which is likely due to an emergence of proteins that are permanently trapped in a fluorescent state (Fig. 2 *A*). Under the employed light conditions each switching cycle was accompanied by ~1% photobleaching. A switched-on ensemble of rsCherry molecules in solution is relatively dim, exhibiting a fluorescence signal corresponding to ~10% of an equally concentrated solution of nonswitchable mCherry. However, the brightness value of a single rsCherry molecule in the on-state is comparable to that of a single mCherry molecule (Table S1 and Fig. S2 in Data S1), which highlights rsCherry's potential for single-molecule-based fluorescence experiments. An ensemble of rsCherry molecules expressed in *E. coli* adopt a thermal equilibrium at which they exhibit 32% of the maximum fluorescence level. Once pushed to its maximum fluorescence brightness, the ensemble relaxes back into thermal equilibrium with a relaxation time of $t_{1/2}^{\text{on}-\text{relax}} \sim 40 \text{ s}$ (Fig. 2 *D*). Under the employed light intensities, the protein shows relatively fast switching kinetics with a $t_{1/2}^{\text{on}} \sim 3 \text{ s}$ and a $t_{1/2}^{\text{off}} \sim 0.05 \text{ s}$. Altogether, rsCherry is a genuine monomeric red fluorescent RSFP with a positive-switching mode.

Reversing the wavelengths required for switching of rsCherry

During the optimization of rsCherry, we found that exchange of a glutamine residue at position 163 against a methionine reversed the effects of the wavelengths that induce the photoswitching. In rsCherry-Gln[163]Met, light of 450 nm builds up the on-state while irradiation with 550 nm, which is also used to probe fluorescence, largely depopulates the fluorescent states. Therefore, rsCherry-Gln[163]Met exhibits a negative-switching mode.

Further rounds of optimization resulted in mCherry-Glu[144]Val, Ser[146]Cys, Ile[161]Ser, Gln[163]Met, Val[177]Phe that maintained a negative switching mode but is improved considerably in the dynamic range of the fluorescence signal between the on- and the off-state (Fig. 2 *B*). We denote this variant rsCherryRev (for reversibly switching Cherry with reversed switching characteristics).

Like mCherry, rsCherryRev is a monomeric protein (Table S1 and Fig. S1 in Data S1). The absorption and fluorescence emission spectra of rsCherryRev and rsCherry in their respective equilibrium states are almost superimposable (Fig. 2 *C*, Table 1). Like rsCherry, in the ensemble of purified proteins, the switched-on rsCherryRev is rather dim, with an on-state ensemble fluorescence signal of ~10% compared to mCherry. Nonetheless, the brightness value of a single rsCherryRev molecule in the on-state is comparable to that of mCherry (Table 1, and Fig. S2 in Data S1) as demonstrated
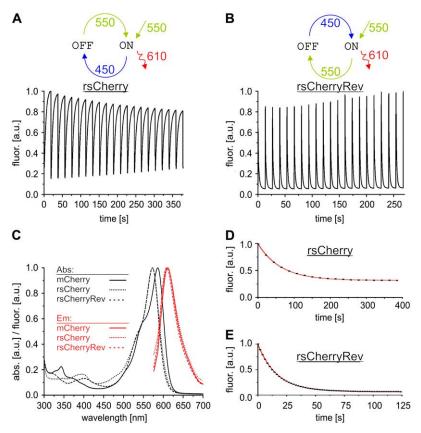
FIGURE 2 Properties of rsCherry and rsCherryRev. (*A and B*) Photoswitching of the fluorescence signal recorded on *E. coli* colonies expressing rsCherry (*A*) or rsCherryRev (*B*). Photoswitching was accomplished by alternating irradiation with yellow light (550 ± 20 nm, 12 s) and yellow together with blue light (450 ± 20 nm, 0.5 s). Yellow light excites fluorescence. (*Graphic* in *A* and *B*) Schematic representation of the respective switching cycles. (*C*) Absorption and emission spectra of mCherry, rsCherry, and rsCherryRev. (*D* and *E*) Relaxation kinetics of rsCherry and rsCherryRev, respectively, from the on-state into the thermal equilibrium state recorded in the dark by consecutive short measurements with yellow light. (*E*) Recorded after several switching cycles (see also Fig. S3 in Data S1). The data points of the relaxation kinetics are fitted to a single-exponential function.

by fluorescence correlation spectroscopy. At thermal equilibrium the fluorescence signal of rsCherryRev is <10% of the maximal attainable signal, hence the majority of the molecules adopt the off-state (Fig. 2 *E*). rsCherryRev displays faster switching kinetics than rsCherry, which is also reflected in its less stable on-state: It relaxes with a relaxation time $t_{1/2}^{\mathrm{on-relax}} \sim 13\,\mathrm{s}$ from the on-state into the thermal equilibrium (Fig. 2 *E*). Interestingly, the relaxation kinetics change when the proteins are repeatedly switched, indicating a complex photophysical behavior involving additional states (Fig. S3 in Data S1). Switched-off rsCherryRev molecules exhibit only 5% of the maximal fluorescence signal, so that rsCherryRev displays a favorable dynamic range of fluorescence switching.

The fluorescence of single *E. coli* colonies on agar plates expressing rsCherryRev may be photoswitched hundreds of times (Fig. 2 *B* and Fig. 3). We found that for the first ~100 switching cycles the recorded maximum fluorescence level increased, while the residual fluorescence in the off-states remained at an almost constant value. For a further ~100 switching cycles, the increase in fluorescence apparently counteracted the photobleaching, before the fluorescence signal decreased (Fig. 3 *A*). The increase of the fluorescence signal during consecutive switching cycles appears to be an irreversible process, since 4 h of darkness during a switching series did not alter the maximal fluorescence (Fig. 3 *B*). This points to a light-induced structural rearrangement of rsCherryRev upon photoswitching. We observed an increase in the fluorescence with successive switching cycles only in rsCherryRev variants containing a cysteine residue at position 146, showing that the mutation Ser[146]Cys is crucial to this phenomenon. The molecular mechanism is, however, unclear.

TABLE 1

	Absorpt. max. (nm)	Emission max. (nm)	Ensemble brightness*	Single-molecule brightness[†]	Switch-on half-time $t_{1/2}^{\mathrm{on}}$ (s)[‡]	Switch-off half-time $t_{1/2}^{\mathrm{off}}$ (s)[‡]	On-state relaxation half-time $t_{1/2}^{\mathrm{on-relax}}$ (s)	Fluor. at equil.	Residual fluor. in the off-state
mCherry	586	611	1	1	n.a.[§]	n.a.[§]	n.a.[§]	100%	n.a.[§]
rsCherry	572	610	~0.1	~1	3.0	0.05	40	32%	15%
rsCherryRev	572	608	~0.1	~1	0.05	0.7	13	8%	5%

*Purified proteins were concentrated to the same 280-nm absorption and fluorescence was measured relative to mCherry.
[†]Determined by fluorescence correlation spectroscopy; the same protein solutions as in the first footnote were used, diluted for the measurements.
[‡]Measured with yellow light 550 ± 20 nm (4 W/cm^{-2}) and blue light 450 ± 20 nm (4 W/cm^2).
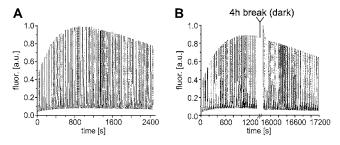[§]Not applicable; mCherry is a nonswitchable protein.

FIGURE 3 rsCherryRev exhibits an increase in the maximal fluorescence signal upon repeated photoswitching. (*A* and *B*) Fluorescence signals of 300 switching cycles recorded on *E. coli* colonies expressing rsCherryRev are shown. Photoswitching was accomplished by alternating irradiation with yellow light (550 ± 20 nm, 12 s) and yellow together with blue light (450 ± 20 nm, 0.5 s). In panel *B*, the switching sequence was interrupted for 4 h after cycle 150.

Hence, rsCherryRev is a bona fide switchable red fluorescent protein with a substantial depth of fluorescence modulation, exhibiting negative-switching for up to several hundred switching cycles in ensemble measurements.

Alternate highlighting of rsCherry and rsCherryRev in *E. coli*

Next, we imaged a mixed culture of *E. coli* cells, expressing either rsCherry or rsCherryRev (Fig. 4). To discriminate between cells expressing the different RSFPs, a sequence of irradiation events bringing them in and out of the on-state was employed. To this end, the cells were first irradiated with light of 546 nm to switch rsCherry on and simultaneously rsCherryRev off. Second, the cells were imaged with 546 nm irradiation and the fluorescence was detected between 580 and 620 nm. In the next step, the sample was irradiated with
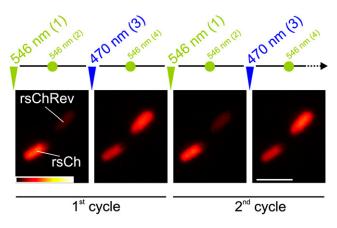

FIGURE 4 Imaging of *E. coli* cells expressing rsCherry or rsCherryRev. The cells were imaged according to the following sequence: 1), Irradiation with yellow light (546 ± 6 nm, 1 s) to switch rsCherry (*rsCh*) in the on-state and rsCherryRev (*rsChRev*) in the off-state. 2), Imaging with yellow light (60 ms). 3), Irradiation with blue light (470 ± 20 nm, 1 s) to switch rsCherry in the off-state and rsCherryRev in the on-state. 4), Imaging with yellow light. Shown are two cycles. Scale bar: 3 μm.

470 nm light to transfer rsCherry into the off-state and rsCherryRev into the on-state. In the last step, the fluorescence signal was recorded as before. Since switching of both proteins is reversible, the imaging sequence could be repeated several times (Fig. 4). Because an ensemble of rsCherry molecules exhibits a residual fluorescence signal after switching off that corresponds to ~15% of its maximum signal (Table 1), the *E. coli* cell expressing rsCherry is clearly visible even when the proteins are switched off. Hence, rsCherryRev, due to its more favorable dynamic range between the on- and the off-state, appears to be more suitable for most imaging applications that rely on photoswitching with good contrast.

Application of rsCherryRev in mammalian cells as a cellular marker

Therefore, we next tested rsCherryRev for its performance when expressed in mammalian cells. To this end we targeted rsCherryRev to the endoplasmic reticulum (ER) by fusing it to an N-terminal ER targeting signal and a C-terminal retention sequence. Cells expressing this construct displayed bright fluorescence and were not affected in their viability (Fig. 5 *A*). The fluorescence was reversibly switchable by irradiating the live cells with blue (495 ± 7.5 nm) and yellow (570 ± 10 nm) light. We also fused rsCherryRev to α-Tubulin resulting in a fluorescently-labeled microtubule network underscoring the fact that rsCherryRev is functionally monomeric (Fig. 5 *A*) and can be readily utilized for imaging applications.

Live-cell PALMIRA

To demonstrate the utility of rsCherryRev for subdiffraction resolution imaging in living mammalian cells, we imaged the rsCherryRev-labeled ER using the PALMIRA mode (12). The intricate ER is a dynamic polygonal array of interconnected tubules that spreads throughout the cell (37,38). The diameter of individual tubules is frequently well below the diffraction barrier and hence many of the features of the reticulum are difficult or even impossible to resolve using conventional far-field microscopy.

To visualize the ER within a living cell we captured 60,000 frames lasting 2 ms each without pause. We divided them into three groups of 20,000 frames to visualize the movement of the ER over the course of the image acquisition period. The resulting effective acquisition time of 40 s per image allowed us to follow movements of the network at the nanoscale (Fig. 5 *B*). Movements taking place within the recording time are averaged out in the resulting image. The chosen frame rate was long enough to capture (in >90% of all events) all detectable photons emitted from a molecule in its temporary fluorescent on-state in one frame. Utilizing all events exhibiting at least 20 photons, the achieved resolution was <75 nm in the optical plane as demonstrated on small structures of the
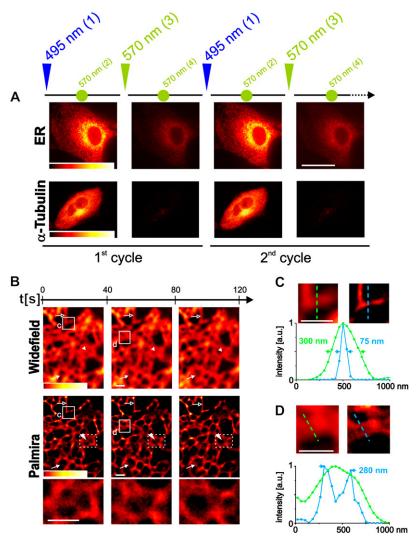
FIGURE 5 Applications of rsCherryRev in live PtK2 cells. (A) Imaging of rsCherryRev targeted to the ER (top row) and an rsCherryRev-α-Tubulin fusion protein (bottom row). Reversible switching was accomplished by consecutive irradiations with 1), blue light (495 ± 7.5 nm, 1.1 s) to switch the protein in the on-state; 2), yellow light (570 ± 10 nm, 160 ms) for imaging; 3), yellow light (570 ± 10 nm, 1.1 s) to switch the protein in the off-state; and, 4), yellow light (570 ± 10 nm, 160 ms) for imaging. The sequence was repeated starting at 1. (B–D) Time-lapse live-cell PALMIRA imaging of cells expressing rsCherryRev targeted to the ER. Conventional (B, top row) and PALMIRA images (B, middle row). The three images were recorded successively on the same living cell. Recording time: 40 s. (Hollow arrows) Unchanged tubule. (Solid arrows) Emerging tubule. (Arrowheads) Disappearing tubule. (B, bottom row) Magnification of the areas marked by rectangles with dotted lines to highlight the changes in the ER meshwork over time. (C and D) Magnification of the areas marked in B with c or d, respectively. (Graphs) Intensity profiles along the indicated dashed lines. Scale bars: 20 μm (A), 1 μm (B–D).

ER (Fig. 5 C). At this resolution, structures of the ER can be delineated at the nanoscale which are not resolvable by conventional microscopy (Fig. 5 D). These results clearly show that rsCherryRev, visualized in the PALMIRA mode, is appropriate to reveal the organization of nanosized organelles within living mammalian cells.

DISCUSSION

In this study, we generated two novel monomeric red fluorescent photoswitchable proteins based on the nonswitchable fluorescent protein mCherry. The new RSFPs rsCherry and rsCherryRev exhibit positive and negative switching modes, respectively. rsCherryRev is suitable for protein labeling in mammalian cells. Targeted to the endoplasmic reticulum, rsCherryRev could be utilized for time-resolved subdiffraction resolution microscopy in living mammalian cells.

The generation of these two novel RSFPs was based on the assumption that a fluorescent protein can be made switchable, provided the chromophore is allowed to undergo a cis-

trans isomerization. In mCherry, the chromophore adopts a cis-conformation and it apparently cannot access the trans-conformation because the required space is occupied by a bulky isoleucine residue. We found that upon exchange of this residue by a smaller serine residue (Ile[161]Ser), the protein gained switching capabilities. This strongly indicates that in rsCherry, which is an improved mCherry-Ile[161]Ser variant, the on-state chromophore adopts a cis-conformation, and the off-state chromophore a trans-conformation.

rsCherry exhibits positive-switching, so that irradiation with yellow light, which also elicits fluorescence, transfers the protein from the off- to the on-state. Blue light induces the reverse switching direction. Introduction of Gln[163]Met reversed the effects of the switching wavelengths, rendering Gln[163]Met the key mutation in rsCherryRev. The mCherry structure suggests that in rsCherryRev the amino-acid residue at position 163 is located between the chromophoric p-hydroxyphenyl ring in the cis- and the hypothetical trans-position. Hence, this residue is in a prime position to influence the chromophore and its immediate environment. Two

explanations as to how the residue exchange Gln^{163}Met may result in a reversion of the wavelengths may be envisioned. First, it may influence the chromophore cavities in a way that irradiation with 450 nm now induces the transition from the *trans*- to the *cis*-conformation and that 550 nm light induces the reverse effect. Alternatively, Gln^{163}Met may render the *cis*-position nonfluorescent and the *trans*-position fluorescent. In the latter case, the direction of the light-induced conformation changes would remain the same as in rsCherry. We found that reintroduction of an isoleucine residue at position 161 into a switchable rsCherryRev variant (mCherry-Glu^{144}Val, Ile^{161}Ser, Gln^{163}Met, Val^{177}Phe) resulted in a nonswitchable, but fluorescent protein (Fig. S4 in Data S1). An isoleucine at position 161 most likely prevents the chromophore from adopting a *trans* conformation. This observation supports the view that in rsCherryRev the on-state chromophore adopts a *cis*-conformation as well. The absorption spectra of rsCherry and rsCherryRev at pH 7.0 displayed a major peak at 572 nm, corresponding to the deprotonated (anionic) state of the chromophore. At pH 5.0, both proteins show an additional absorption peak at 464 nm (Fig. S5 in Data S1), corresponding to the neutral state (1,39). Altogether, these findings strongly support the view that the switching mechanism of rsCherry and rsCherryRev follows similar lines as described for other RSFPs (16,17,21). The irradiation with blue light apparently induces the conversion from a little populated neutral *cis*-(rsCherry) or *trans*-(rsCherryRev) state, respectively, into the corresponding other state. Irradiation with yellow light induces the isomerization from the predominantly deprotonated *trans*-(rsCherry) or *cis*-(rsCherryRev) state in the other direction.

Both rsCherry and rsCherryRev display rather low ensemble but excellent single-molecule brightness values compared to mCherry. We found that chromophore maturation appears to be only slightly diminished in rsCherry and rsCherryRev, as compared to mCherry (to ~40% and ~70%, respectively; see Fig. S6 in Data S1). Therefore, at least under the wide-field illumination that is used to determine the ensemble brightnesses, an incomplete activation, potentially due to competing transitions into other nonfluorescent states, is likely to explain a substantial part of the reduced ensemble brightness values of rsCherry and rsCherryRev. Possibly, the activation is more efficient using high light intensities, which would explain the unexpected bright images (Fig. 5 *A*) when using more intense irradiation.

In this study, we demonstrated the utilization of rsCherryRev for time-lapse live-cell subdiffraction microscopy based on the switching and localization of single-molecule emitters. rsCherryRev, like its relative rsCherry, has been generated by mutagenesis on the basis of a previously well-characterized nonswitchable fluorescent protein. It can easily be envisioned that further RSFPs with diverse photophysical properties may be generated along the mutagenesis strategies outlined here. Hence, the addition of the now available red RSFPs may initiate a collection of reversibly switchable fluorescent proteins glowing in all hues that will foster new developments in live-cell multicolor subdiffraction resolution microscopy, based on RESOLFT (13,29) or single-molecule superresolution concepts and related schemes (10,12,30,31), to address a multitude of problems in cell biology.

SUPPLEMENTARY MATERIAL

To view all of the supplemental files associated with this article, visit www.biophysj.org.

REFERENCES

1. Tsien, R. Y. 1998. The green fluorescent protein. *Annu. Rev. Biochem.* 67:509–544.

2. Matz, M. V., A. F. Fradkov, Y. A. Labas, A. P. Savitsky, A. G. Zaraisky, M. L. Markelov, and S. A. Lukyanov. 1999. Fluorescent proteins from nonbioluminescent *Anthozoa* species. *Nat. Biotechnol.* 17:969–973.

3. Shaner, N. C., R. E. Campbell, P. A. Steinbach, B. N. Giepmans, A. E. Palmer, and R. Y. Tsien. 2004. Improved monomeric red, orange and yellow fluorescent proteins derived from *Discosoma* sp. red fluorescent protein. *Nat. Biotechnol.* 22:1567–1572.

4. Lukyanov, K. A., A. F. Fradkov, N. G. Gurskaya, M. V. Matz, Y. A. Labas, A. P. Savitsky, M. L. Markelov, A. G. Zaraisky, X. N. Zhao, Y. Fang, W. Y. Tan, and S. A. Lukyanov. 2000. Natural animal coloration can be determined by a nonfluorescent green fluorescent protein homolog. *J. Biol. Chem.* 275:25879–25882.

5. Ando, R., H. Mizuno, and A. Miyawaki. 2004. Regulated fast nucleocytoplasmic shuttling observed by reversible protein highlighting. *Science.* 306:1370–1373.

6. Chudakov, D. M., T. V. Chepurnykh, V. V. Belousov, S. Lukyanov, and K. A. Lukyanov. 2006. Fast and precise protein tracking using repeated reversible photoactivation. *Traffic.* 7:1304–1310.

7. Eggeling, C., M. Hilbert, H. Bock, C. Ringemann, M. Hofmann, A. C. Stiel, M. Andresen, S. Jakobs, A. Egner, A. Schonle, and S. W. Hell. 2007. Reversible photoswitching enables single-molecule fluorescence fluctuation spectroscopy at high molecular concentration. *Microsc. Res. Tech.* 70:1003–1009.

8. Hell, S. W., S. Jakobs, and L. Kastrup. 2003. Imaging and writing at the nanoscale with focused visible light through saturable optical transitions. *Appl. Phys. A Mat.* 77:859–860.

9. Hofmann, M., C. Eggeling, S. Jakobs, and S. W. Hell. 2005. Breaking the diffraction barrier in fluorescence microscopy at low light intensities by using reversibly photoswitchable proteins. *Proc. Natl. Acad. Sci. USA.* 102:17565–17569.

10. Betzig, E., G. H. Patterson, R. Sougrat, O. W. Lindwasser, S. Olenych, J. S. Bonifacino, M. W. Davidson, J. Lippincott-Schwartz, and H. F. Hess. 2006. Imaging intracellular fluorescent proteins at nanometer resolution. *Science.* 313:1642–1645.

11. Dedecker, P., J. Hotta, C. Flors, M. Sliwa, H. Uji-i, M. B. Roeffaers, R. Ando, H. Mizuno, A. Miyawaki, and J. Hofkens. 2007. Subdiffraction imaging through the selective donut-mode depletion of thermally stable photoswitchable fluorophores: numerical analysis

and application to the fluorescent protein Dronpa. *J. Am. Chem. Soc.* 129:16132–16141.

12. Egner, A., C. Geisler, C. von Middendorff, H. Bock, D. Wenzel, R. Medda, M. Andresen, A. C. Stiel, S. Jakobs, C. Eggeling, A. Schonle, and S. W. Hell. 2007. Fluorescence nanoscopy in whole cells by asynchronous localization of photoswitching emitters. *Biophys. J.* 93:3285–3290.

13. Hell, S. W. 2007. Far-field optical nanoscopy. *Science.* 316:1153–1158.

14. Lukyanov, K. A., D. M. Chudakov, S. Lukyanov, and V. V. Verkhusha. 2005. Innovation: photoactivatable fluorescent proteins. *Nat. Rev. Mol. Cell Biol.* 6:885–891.

15. Chudakov, D. M., A. V. Feofanov, N. N. Mudriku, S. Lukyanov, and K. A. Lukyanov. 2003. Chromophore environment provides clue to ''kindling fluorescent protein'' riddle. *J. Biol. Chem.* 278:7215–7219.

16. Andresen, M., M. C. Wahl, A. C. Stiel, F. Gräter, L. V. Schäfer, S. Trowitzsch, G. Weber, C. Eggeling, H. Grubmüller, S. W. Hell, and S. Jakobs. 2005. Structure and mechanism of the reversible photoswitch of a fluorescent protein. *Proc. Natl. Acad. Sci. USA.* 102:13070–13074.

17. Andresen, M., A. C. Stiel, S. Trowitzsch, G. Weber, C. Eggeling, M. C. Wahl, S. W. Hell, and S. Jakobs. 2007. Structural basis for reversible photoswitching in Dronpa. *Proc. Natl. Acad. Sci. USA.* 104:13005–13009.

18. Stiel, A. C., S. Trowitzsch, G. Weber, M. Andresen, C. Eggeling, S. W. Hell, S. Jakobs, and M. C. Wahl. 2007. 1.8 A bright-state structure of the reversibly switchable fluorescent protein Dronpa guides the generation of fast switching variants. *Biochem. J.* 402:35–42.

19. Henderson, J. N., H. W. Ai, R. E. Campbell, and S. J. Remington. 2007. Structural basis for reversible photobleaching of a green fluorescent protein homologue. *Proc. Natl. Acad. Sci. USA.* 104:6672–6677.

20. Habuchi, S., R. Ando, P. Dedecker, W. Verheijen, H. Mizuno, A. Miyawaki, and J. Hofkens. 2005. Reversible single-molecule photoswitching in the GFP-like fluorescent protein Dronpa. *Proc. Natl. Acad. Sci. USA.* 102:9511–9516.

21. Habuchi, S., P. Dedecker, J. Hotta, C. Flors, R. Ando, H. Mizuno, A. Miyawaki, and J. Hofkens. 2006. Photo-induced protonation/deprotonation in the GFP-like fluorescent protein Dronpa: mechanism responsible for the reversible photoswitching. *Photochem. Photobiol. Sci.* 5:567–576.

22. Schäfer, L. V., G. Groenhof, A. R. Klingen, G. M. Ullmann, M. Boggio-Pasqua, M. A. Robb, and H. Grubmüller. 2007. Photoswitching of the fluorescent protein asFP595: mechanism, proton pathways, and absorption spectra. *Angew. Chem. Int. Ed.* 46:530–536.

23. Cinelli, R. A. G., V. Pellegrini, A. Ferrari, P. Faraci, R. Nifosi, M. Tyagi, M. Giacca, and F. Beltram. 2001. Green fluorescent proteins as optically controllable elements in bioelectronics. *Appl. Phys. Lett.* 79:3353–3355.

24. Ando, R., C. Flors, H. Mizuno, J. Hofkens, and A. Miyawaki. 2007. Highlighted generation of fluorescence signals using simultaneous two-color irradiation on Dronpa mutants. *Biophys. J.* 92:L97–L99.

25. Chudakov, D. M., V. V. Belousov, A. G. Zaraisky, V. V. Novoselov, D. B. Staroverov, D. B. Zorov, S. Lukyanov, and K. A. Lukyanov. 2003. Kindling fluorescent proteins for precise in vivo photolabeling. *Nat. Biotechnol.* 21:191–194.

26. Hell, S. W., and J. Wichmann. 1994. Breaking the diffraction resolution limit by stimulated emission: stimulated emission depletion microscopy. *Opt. Lett.* 19:780–782.

27. Klar, T. A., S. Jakobs, M. Dyba, A. Egner, and S. W. Hell. 2000. Fluorescence microscopy with diffraction resolution barrier broken by stimulated emission. *Proc. Natl. Acad. Sci. USA.* 97:8206–8210.

28. Hell, S. W. 2003. Toward fluorescence nanoscopy. *Nat. Biotechnol.* 21:1347–1355.

29. Hell, S. W., M. Dyba, and S. Jakobs. 2004. Concepts for nanoscale resolution in fluorescence microscopy. *Curr. Opin. Neurobiol.* 14:599–609.

30. Rust, M., M. Bates, and X. Zhuang. 2006. Sub-diffraction-limit imaging by stochastic optical reconstruction microscopy (STORM). *Nat. Methods.* 3:793–795.

31. Hess, S. T., T. P. Girirajan, and M. D. Mason. 2006. Ultra-high resolution imaging by fluorescence photoactivation localization microscopy. *Biophys. J.* 91:4258–4272.

32. Sawano, A., and A. Miyawaki. 2000. Directed evolution of green fluorescent protein by a new versatile PCR strategy for site-directed and semi-random mutagenesis. *Nucleic Acids Res.* 28:E78.

33. Leung, D. W., E. Chen, and D. V. Goeddel. 1989. A method for random mutagenesis of a defined DNA segment using a modified polymerase chain reaction. *Technique.* 1:11–15.

34. Magde, D., E. Elson, and W. W. Webb. 1972. Thermodynamic fluctuations in a reacting system: measurement by fluorescence correlation spectroscopy. *Phys. Rev. Lett.* 29:705–708.

35. Hogbom, J. A. 1974. Aperture synthesis with a non-regular distribution of interferometer baselines. *Astron. Astrophys. Supp.* 15:417–426.

36. Shu, X., N. C. Shaner, C. A. Yarbrough, R. Y. Tsien, and S. J. Remington. 2006. Novel chromophores and buried charges control color in mFruits. *Biochemistry.* 45:9639–9647.

37. Baumann, O., and B. Walz. 2001. Endoplasmic reticulum of animal cells and its organization into structural and functional domains. *Int. Rev. Cytol.* 205:149–214.

38. Lee, C., and L. B. Chen. 1988. Dynamic behavior of endoplasmic reticulum in living cells. *Cell.* 54:37–46.

39. Yampolsky, I. V., S. J. Remington, V. I. Martynov, V. K. Potapov, S. Lukyanov, and K. A. Lukyanov. 2005. Synthesis and properties of the chromophore of the asFP595 chromoprotein from Anemonia sulcata. *Biochemistry.* 44:5788–5793.